

# DEEP LEARNING BASED MULTI TASK ROAD EXTRACTOR MODEL FOR PARCEL EXTRACTION AND CROP CLASSIFICATION USING KNOWLEDGE BASED NDVI TIME SERIES DATA

Ammar Dali<sup>1</sup>, Kamal Jain<sup>1</sup>, Siddhartha Khare<sup>1</sup>, Sunni Kanta Prasad Kushwaha<sup>1</sup>

<sup>1</sup> Department of Civil Engineering, Indian Institute of Technology Roorkee, Uttarakhand, India

**KEY WORDS:** Edge Detection, Parcel Delineation, Deep Learning, Crop Classification, NDVI

## ABSTRACT:

The role of agriculture in food security is critical by the rapid increase of the global population. Food production should be strongly increased to secure and provide life necessities. Remote sensing provides a fruitful tool in agriculture management, and it provides advantages in terms of saving time and effort. This study aims to examine the feasibility of deep learning edge detection algorithm in order to automatically extract the agricultural parcel boundaries from the open-source Google Earth data. The potential of using Normalized Difference Vegetation Index (NDVI) in crop classification crop was also presented after analyzing the pattern of Rabi major crops (Wheat and Sugarcane) in Haridwar district, Uttarakhand, India. The advantage of Google Earth Engine cloud-based platform was exploited in generating NDVI data from Sentinel-2 satellite between October 2022 and February 2023 in order to save time and effort. To check the accuracy of the deep learning model, the value of the Mean Intersection of Union (mIoU) was tested and reached 0.79. To examine the results, ground truth data were collected in the study area using Unmanned Aerial Vehicles. The overall accuracy of the rule set-based classification reached 91.17%, and the kappa coefficient value was 0.82.

## 1. INTRODUCTION

The 2.3 billion people increase in global population is playing a significant role in the rapid increase of global food necessities from agricultural crops (Tilman *et al.*, 2011). The anticipation that the global population by 2050 is around 9.8 billion; thus, measures should be taken such as increasing food production (Tilman *et al.*, 2011). The reports indicate that around 1 billion people suffer from famine every day as a result of the lack of food supply, and this number is to be increased by 2050 to 2 billion. According to this storyline, agriculture production should be enforced to be increased by 70% in African and Asian developing countries in the future (FAO, 2009). Since the beginning of the 1970's, remotely sensed data provided by satellites have been adopted to be used in agriculture (Tempfli *et al.*, 2013; Mulla, 2013). At the large-scale regions, remote sensing techniques with effective spatial and temporal information play a significant role as an important factor in the management of agricultural fields and crop monitoring (Gao *et al.*, 2017). In order to automatically extract the cadastral information from remotely sensed data, deep learning methodology was adopted in many applications, such as road extraction, object extraction, parcel delineation, etc. In terms of agriculture, deep learning techniques is used recently to extract the agricultural parcel boundaries as the manual methods represented by digitization is time and effort-consuming. Notable number of studies used the conventional supervised classification to extract the crop information using only one single image. Because of crop variability and pixel heterogeneity, the application of traditional pixel-based classification techniques is limited as a result of the "salt and pepper" effect. The spectral similarity between various crops can be avoided by analyzing time series data provided by space platforms (Li *et al.*, 2015a). The basic idea of remote sensing of vegetation is acquiring information on the interaction between

electromagnetic energy and vegetation on the surface of the earth via passive sensors. Many factors play an important role in the difference in the reflectance of electromagnetic spectra, such as plant class, water content, etc. (Mulla, 2013; Liu, Sun and Liu, 2016). For the process of many quantitative and qualitative evaluations, such as growth dynamics, vegetation cover, and vigor, the derived vegetation indices from remote sensing-based canopies are straightforward and widely used. The remote sensed spectral characteristics and information from the canopy and plants are obtained by the differences in the green leaves (Xue and Su, 2017). Normalized Difference Vegetation Index (NDVI) is one of the most widely used in multi-spectral remote sensing, and it is derived by dividing the difference between red and near-infrared bands on the sum of them (Karnieli *et al.*, 2010; Yin *et al.*, 2012; Jain and Pandey, 2021; Pandey and Jain, 2022). NDVI is used in many applications, such as health condition assessment and deforestation analysis (Singh and Kushwaha, 2021; Yogender *et al.*, 2022). As long as the NDVI value is positive, the class is crops, grass, forests, and other vegetation cover, in contrast, the negative values indicate non-vegetation cover such as urban area, sand rocks, etc. (Pettorelli *et al.*, 2005). The major problem in remotely sensed image classification is the crop variability represented by the pixel-level spectral heterogeneity which is the source of the pixel-based classification techniques limitation as the "salt and pepper" phenomena is common in the crop pixel-based classification (Vieira *et al.*, 2012; Hu *et al.*, 2013; Li *et al.*, 2015b). The fundamental requirement for conventional supervised image classification approaches is collecting training data (Tempfli *et al.*, 2013). According to (Huang, Davis and Townshend, 2010) the imbalance of the training samples could affect the quality of the classification; in addition, the effect of training samples might be more than the algorithm used itself. In this study, the feasibility of deep learning methods was examined in order to automatically extract the

cadastral agricultural field using the free availability of Google Earth Data, then the capability of time series NDVI extracted from Sentinel-2 satellite with the synergistic of the Google Earth Engine cloud-based platform was tested to extract the major Rabi crops (Sugarcane and Wheat) in Haridwar district, India.

## 2. STUDY AREA AND DATA USED

### 2.1 Study Area

Haridwar district is a part of Uttarakhand state in northern India. The area of Haridwar is around 2360 sq km between 29°35' N to 30°40' N and 77°43' E to 78°22' E. The district has a hot sub-humid (dry) eco-region climate with a moderate to humid sub-tropical climate. Monsoon is the rainy season in Haridwar with annual precipitation of 1174.3 mm approximately (Ministry of Water Resources, 2016). The main cereal crop during the Kharif season for more than 54% of Uttarakhand's total cultivated area is rice with a 115-120 days life cycle, Sugarcane is the predominant crop in Uttarakhand, India, and has around 84 thousand hectares (Korikanthmath, Manjunath and Manohara, 2010; Kumar, Kashyap and Tyagi, 2018). The most predominant cultivated crop in the highlands of Uttarakhand state-north India is Wheat; moreover, its growth cycle extends between 180-210 days in which the sowing time is November-December and the harvesting time is April- May. The study has been carried out in a small experimental area near Sirchandi located between 77° 44' E to 77°45' E and 29°55' N to 29°56' N. The study area and experimental area are shown in Figure 1.

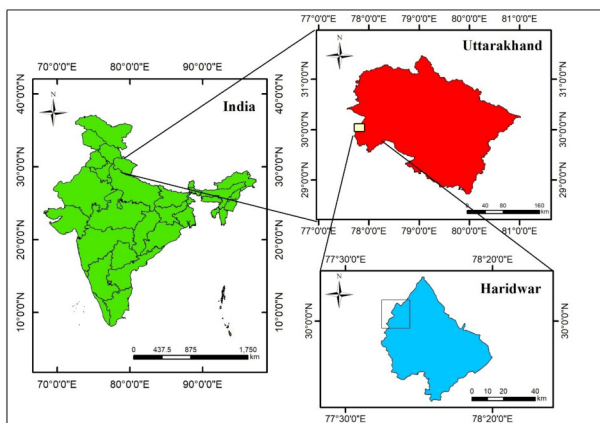


Figure 1. Study Area

### 2.2 Data Used

#### 2.2.1 Google Earth Data

Google Earth is a popular geospatial tool developed by Google that allows users to explore the Earth's surface using satellite imagery, aerial photography, and 3D models. Since its launch in 2005, Google Earth has been widely used in various fields, such as geography, environmental science, urban planning, and archaeology.

In this investigation, a patch of the latest image of the study area was collected from Google Earth on the date of 24<sup>th</sup> November 2022. The procedure of exporting the image was done using the Save Image tool available in Google Earth software with the maximum resolution (1529\*925), after exporting the image from Google Earth, it was imported to ArcGIS in order to relate the

internal coordinate system of a that digital map to a ground system geographic coordinates. Georeferencing was conducted in GIS environment. The image shows the boundary between the agriculture parcels in Rabi season when the season of harvesting period is already done, and the boundaries between agriculture parcels are easily interpreted. The Google Earth image of the study area is shown in Figure 2.

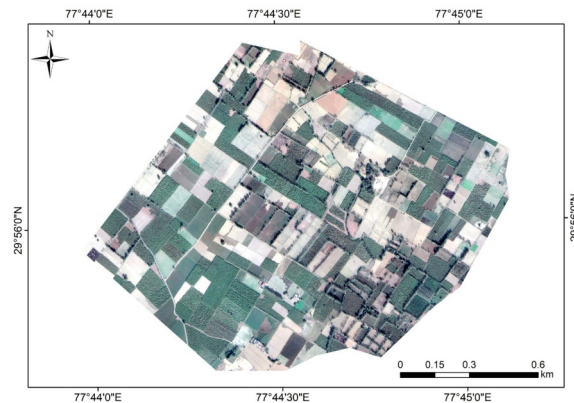


Figure 2. Google Earth Image of the Study Area

#### 2.2.2 Sentinel-2 Data

The advantage of 10 m medium spatial resolution of Sentinel-2 multispectral satellite was exploited in this study in order to classify the crop types in the study area.

The feasibility of Google Earth Engine platform were used in order to collect the NDVI data during the study period. Google Earth Engine is a geospatial processing online platform saves time and effort.

## 3. METHODOLOGY WORKFLOW

Google Earth image was downloaded as an input to generate the boundaries between the agriculture parcels. The next step of the investigation is to apply the knowledge based in order to perform the crop type identification based on time series NDVI data extracted from Sentinel 2. Figure 3 illustrates the methodology workflow.

### 3.1 Data Acquisition

In this investigation, Sentinel-2 Level 2A cloud-free data were collected between October 2022 and February 2023, with the exception of data from January 2023, as the cloud cover was dressing the entire data from this month. The advantages of Google earth Engine platform were exploited in order to save time and effort in data preparation as the conventional methods using available software is time-consuming; as a result, a code was processed on Google Earth Engine in order to obtain the time series NDVI data directly for each month from October 2022 to February 2023.

No	Sensor	Level	Tile ID	Date
1	S2B	2A	T43RGP	16-October-2022
2	S2A	2A	T43RGP	20-November-2022
3	S2B	2A	T43RGP	05-December-2022
4	S2B	2A	T43RGP	13-February-2023

Table 2. Data Used

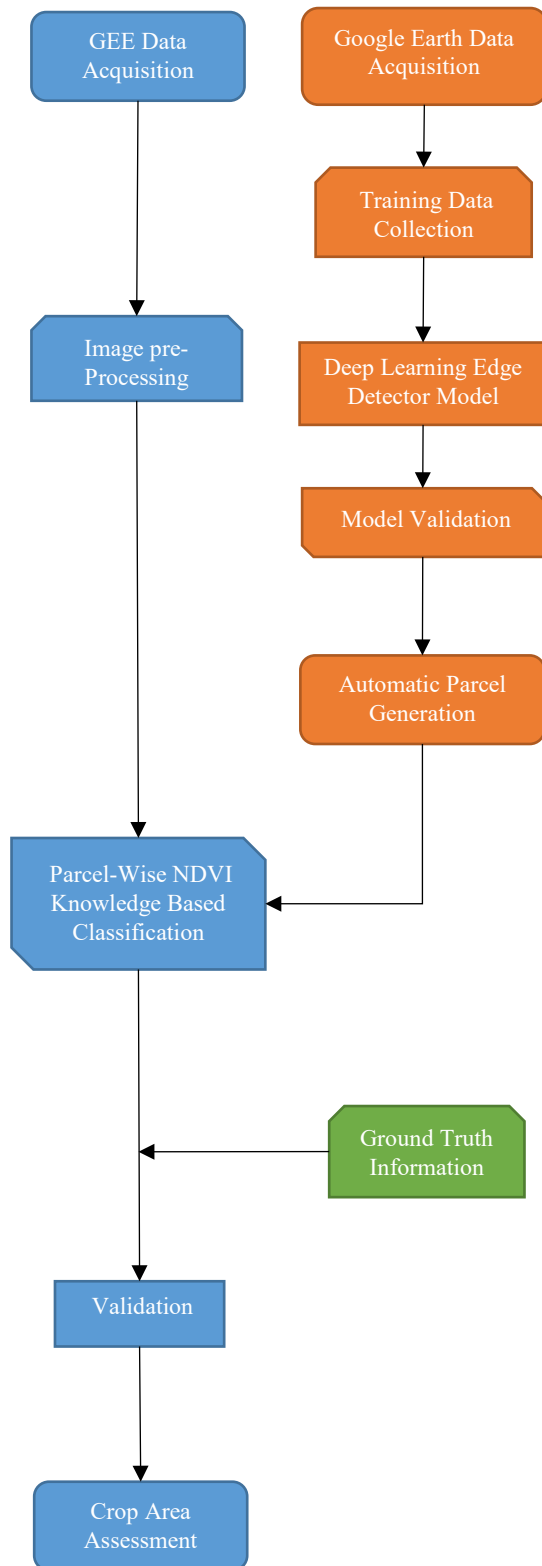


Figure 3. Methodology Flow Chart

NDVI data is downloaded with the help of Google Earth Engine platform. Figure 4 shows the calculated NDVI from the satellite image.

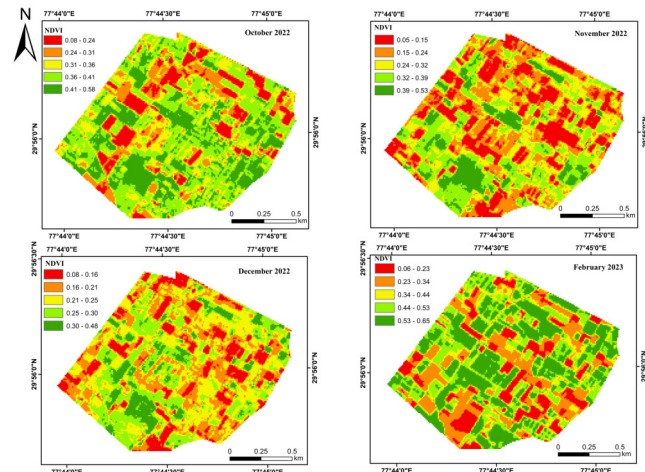


Figure 4. NDVI of the Study Area

### 3.2 Parcel Delineation

After downloading the patch from Google Earth, clipping procedures were implemented in the experimental area. In order to obtain the agricultural cadastral information of the study area, an automated parcel delineation process was performed with the assistance of deep learning methods available on ArcGIS Pro. The deep learning model was performed after collecting training data and performing data training.

### 3.3 Crop Type Extraction

After research and investigation regarding the agricultural condition, an NDVI fixed value of 0.2 has been adopted as a No-Crop Field (Bare Soil) (*NDVI EOS Data Analytics*). According to the crop calendar of Uttarakhand state (*Ministry of Water Resources, 2016*), the harvesting season of rice starts in October-November, which indicates that the field is empty without any crop in this particular period; in addition, wheat crop cultivation usually starts in October-November and harvesting season in April. The threshold values for vegetation and non-vegetation objects were estimated using NDVI. The NDVI threshold value for vegetation was  $> 0.25$ . This threshold value was used to discriminate between vegetation and non-vegetation objects. According to this calendar, the rule set was framed to extract the crop type and it is shown in Table 3.

Crop	NDVI Condition
Wheat	November $< 0.2$ & February $> 0.2$
Sugarcane	November $> 0.2$ & February $> 0.2$

Table 3. Knowledge-Based Logic

## 4. RESULTS AND DISCUSSION

### 4.1 Automatic Parcel Generation

The experiments of parcel extraction and delineation were carried out in GIS environment software. The model was trained using training data collected from Google Earth from the boundaries of the agricultural fields. The number of epochs used to carry out the training procedure was 50 epochs. The ground truth and prediction of the trained model are shown in Figure 5.

The training and validation of each epoch are shown in Figure 6. In order to evaluate the classification results of the model, the value of the Mean Intersection of Union (mIoU) was tested and reached 0.79. mIoU is a widely used evaluation metric in the semantic segmentation task, indicating how accurately each pixel of the image is classified

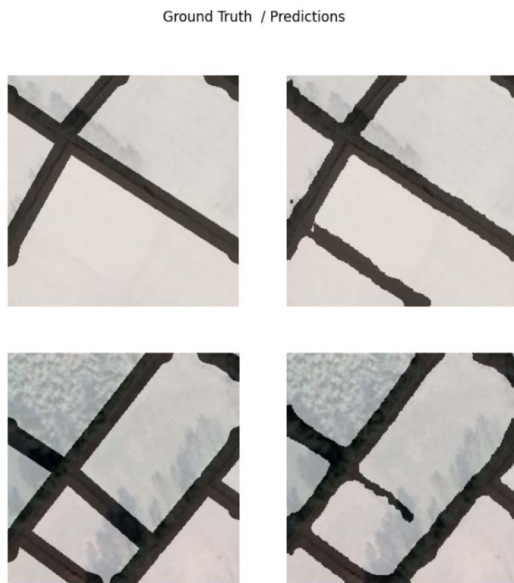


Figure 5. Samples Results

Using GIS environment, the generation of the parcels was done, and the most proper shapes were automatically generated. The final and complete shape of the generated parcels is presented in Figure 7. The result of edge detection between crop and non-crop parcels was shown in Figure 7a, and the edge detection results between crop parcels was shown in Figure 7b.

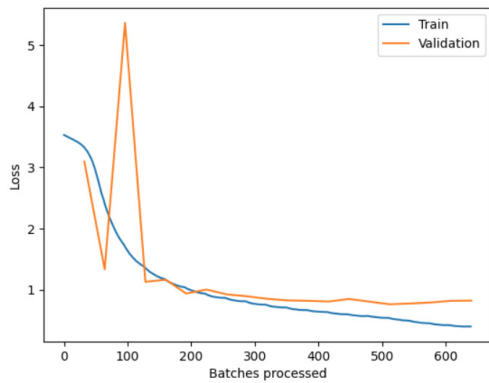
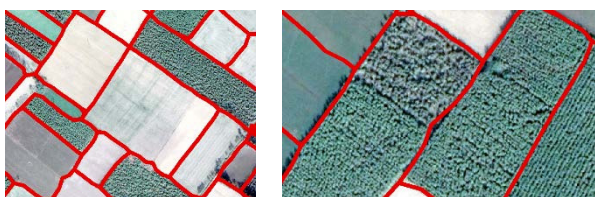


Figure 6. Training and Validation loss



a. Edge Detection between crop and non-crop fields  
 b. Edge Detection between crop fields

Figure 7. Parcels Delineation Results

The visual appearance of the extracted parcels is suitable and satisfying. The final results of parcel delineation is shown in Figure 8 after processing in GIS environment.

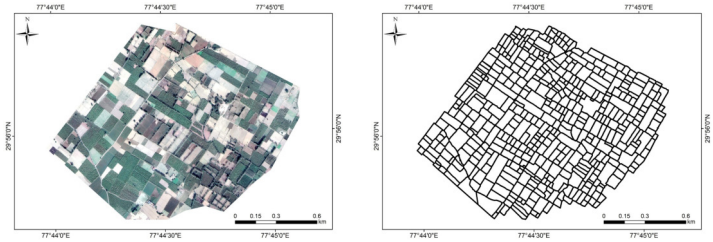


Figure 8. Final Parcels Delineation Results

### 4.2 NDVI Parcel Mean Generation

After exporting the NDVI data from GEE platform, a model was formed using modeling functions and GIS capabilities on ArcGIS software to prepare the NDVI time series data for the span of time. NDVI value was calculated for every parcel using GIS tools. Figure 4 shows the calculated NDVI from the satellite image; meanwhile, Figure 9 shows the mean value (parcel-wise) which is generated based on the automated parcels delineation.

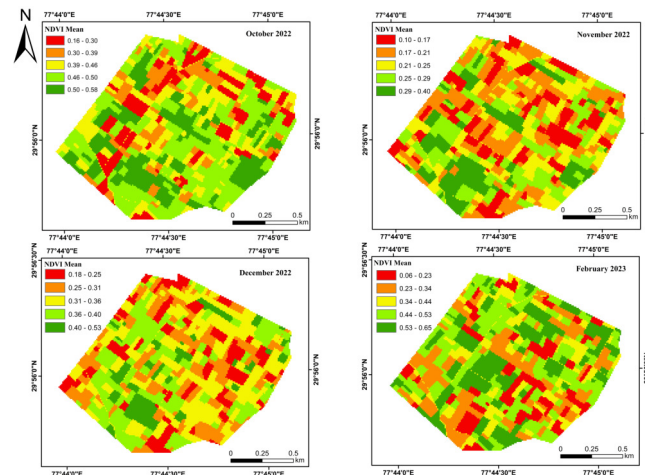


Figure 9. Mean NDVI of the Study Area

### 4.3 Crop Classification

After applying the logic to the study area, the knowledge-Based crop classification results are shown in Figure 10. The harvesting stage of sugarcane usually commences in the middle of March to April. In this study, the period was during the stage of sugarcane maturity; as a result, NDVI value was high during the period between November-February. For the crop of wheat, cultivation starts in October-November, in context the maturity of this crop in January-February. Figure 11 is shown the pattern of NDVI values during the study time period.

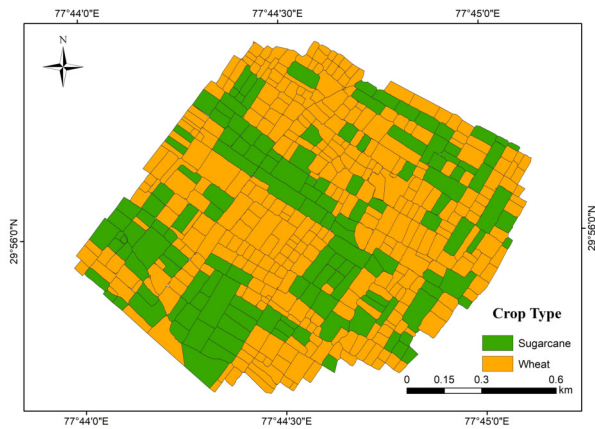


Figure 10. Crop Classification Map

Figure 11 shows the NDVI pattern of crops by plotting the average values of 5 parcels in the study area.

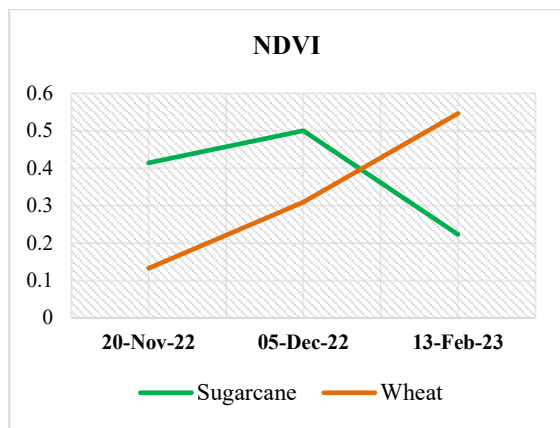


Figure 11. NDVI Trajectory of Crop

#### 4.4 Crop Area Assessment

According to the knowledge-Based classification, the crop area was assessed for both sugarcane and wheat. Figure 12 is presented the area of sugarcane, which reached 731250.3 sq m; in contrast, the area of wheat reached 751350 sq m.

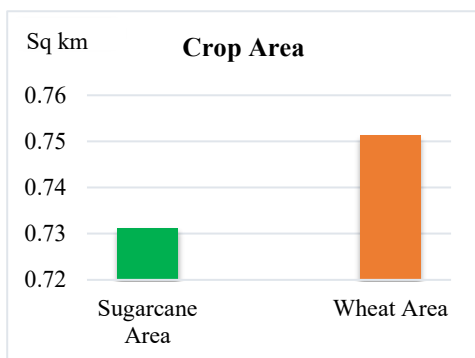


Figure 12. Crop Area

#### 4.5 Accuracy Assessment of the Crop Classification

In order to check the accuracy of the knowledge-Based crop classification, ground truth data were collected from the study

area on the date of 03<sup>rd</sup> April 2023. The ground truth data were a combination of points collected from an RGB image acquired using UAV (Unmanned Aerial Vehicle) over the study area and the same Google Earth Image which was in the date of 24<sup>th</sup> November 2022 (Sugarcane was presented from November to March-April as per the crop calendar). The major crops in Rabi season in the study area are sugarcane and wheat; in this context, both crops are easily identified from UAV RGB images. The number of testing data is shown in Table 4 and the UAV image is shown in Figure 13.

Class	Number of Reference Data
Sugarcane	15
Wheat	19

Table 4. Reference Data



Figure 13. UAV RGB Image of Study Area

The confusion matrix is shown in Table 5. The error matrix is shown in Table 5, the overall accuracy of the knowledge-based classification reached 91.17%, and the kappa coefficient value is 0.82, which indicates the good performance of the classification. Producer's Accuracies were as the following: 93.3% and 89.47% Sugarcane and Wheat, respectively; meanwhile, the User's Accuracies of our classification were as the following: 87.5% and 94.4% of Sugarcane and Wheat.

	Sugarcane	Wheat	Total	UA %
Sugarcane	14	2	16	87.5
Wheat	1	17	18	94.4
Total	15	19		
PA %	93.3	89.47		
OA %	91.17			
Kappa	0.82			

Table 5. Confusion Matrix

## 5. CONCLUSION

This study presented the potential of using the deep learning algorithms to automatically delineate the agricultural cadastral parcels from Google Earth open source data. For crop identification, the investigation highlighted the feasibility of using knowledge-based times series of Normalized Difference Vegetation Index (NDVI) in crop classification compared to conventional methods represented by normal machine learning

classification algorithms based on one single image, which leads to uncertainty and misclassification due to salt and paper impact. Analyzing the NDVI trajectory and pattern of each crop was conducted in this study before performing the knowledge-based crop classification. The results of the parcel delineation were satisfactory and visually interpreted after comparison with the RGB image provided by Google Earth. After validation with ground truth data, the accuracy assessment of the knowledge-based classification reached 91.17% and Kappa coefficient value was 0.82. However, the drawback of this framework was represented by the limitation of the availability of updated data from Google Earth which as the parcels boundaries don't remain as the same status for every season which lead to uncertainty in crop classification, in addition, the process of reshape some cadastral parcels which leads to manual interference of the user to fix some boundaries. This work was done using the Multi Task Road Extractor Model, other models should be examined in the future such as SAM (Segment Anything Model), also the feasibility of other deep learning models for parcel extraction should be on larger scales in different places should also be included in the future work.

## REFERENCES

- FAO (2009) 'How to Feed the World', *How to Feed the World*, pp. 46–58. Available at: <https://doi.org/10.5822/978-1-61091-885-5>.
- Gao, F. *et al.* (2017) 'Toward mapping crop progress at field scales through fusion of Landsat and MODIS imagery', *Remote Sensing of Environment*, 188, pp. 9–25. Available at: <https://doi.org/10.1016/j.rse.2016.11.004>.
- Hu, Q. *et al.* (2013) 'Exploring the use of google earth imagery and object-based methods in land use/cover mapping', *Remote Sensing*, 5(11), pp. 6026–6042. Available at: <https://doi.org/10.3390/rs5116026>.
- Huang, C., Davis, L.S. and Townshend, J.R.G. (2010) 'An assessment of support vector machines for land cover classification', <https://doi.org/10.1080/01431160110040323>, 23(4), pp. 725–749. Available at: <https://doi.org/10.1080/01431160110040323>.
- Jain, K. and Pandey, A. (2021) 'Calibration of Satellite Imagery with Multispectral UAV Imagery', *Journal of the Indian Society of Remote Sensing*, 49(3), pp. 479–490. Available at: <https://doi.org/10.1007/s12524-020-01251-z>.
- Karnieli, A. *et al.* (2010) 'Use of NDVI and land surface temperature for drought assessment: Merits and limitations', *Journal of Climate*, 23(3), pp. 618–633. Available at: <https://doi.org/10.1175/2009JCLI2900.1>.
- Korikanthmath, V.S., Manjunath, B.L. and Manohara, K.K. (2010) 'Status Paper on Rice in Uttarakhand', *ICAR Research Complex For Goa*, p. 23.
- Kumar, S., Kashyap, S. and Tyagi, V.K. (2018) 'Technological options to enhance sugarcane production in plains of Uttarakhand', pp. 1873–1874.
- Li, Q. *et al.* (2015a) 'Object-based crop classification with Landsat-MODIS enhanced time-series data', *Remote Sensing*, 7(12), pp. 16091–16107. Available at: <https://doi.org/10.3390/rs71215820>.
- Li, Q. *et al.* (2015b) 'Object-Based Crop Classification with Landsat-MODIS Enhanced Time-Series Data'. Available at: <https://doi.org/10.3390/rs71215820>.
- Liu, C., Sun, P. Sen and Liu, S.R. (2016) 'A review of plant spectral reflectance response to water physiological changes', *Chinese Journal of Plant Ecology*, 40(1), pp. 80–91. Available at: <https://doi.org/10.17521/cjpe.2015.0267>.
- Ministry of Water Resources (2016) 'Uttarakhand Region, Dehradun'. Available at: [http://cgwb.gov.in/AQM/NAQUIM\\_REPORT/Uttarakhand/Haridwar.pdf](http://cgwb.gov.in/AQM/NAQUIM_REPORT/Uttarakhand/Haridwar.pdf).
- Mulla, D.J. (2013) 'Twenty five years of remote sensing in precision agriculture: Key advances and remaining knowledge gaps', *Biosystems Engineering*, 114(4), pp. 358–371. Available at: <https://doi.org/10.1016/j.biosystemseng.2012.08.009>.
- NDVI (EOS Data Analytics) (no date). Available at: <https://eos.com/blog/ndvi-faq-all-you-need-to-know-about-ndvi/>.
- Pandey, A. and Jain, K. (2022) 'A robust deep attention dense convolutional neural network for plant leaf disease identification and classification from smart phone captured real world images', *Ecological Informatics*, 70(July 2021), p. 101725. Available at: <https://doi.org/10.1016/j.ecoinf.2022.101725>.
- Pettorelli, N. *et al.* (2005) 'Using the satellite-derived NDVI to assess ecological responses to environmental change', *Trends in Ecology and Evolution*, 20(9), pp. 503–510. Available at: <https://doi.org/10.1016/j.tree.2005.05.011>.
- Singh, A. and Kushwaha, S.K.P. (2021) 'Forest Degradation Assessment Using UAV Optical Photogrammetry and SAR Data', *Journal of the Indian Society of Remote Sensing*, 49(3), pp. 559–567. Available at: <https://doi.org/10.1007/s12524-020-01232-2>.
- Tempfli, K. *et al.* (2013) 'Principles of Remote Sensing', *AGERE! 2013 - Proceedings of the 2013 ACM Workshop on Programming Based on Actors, Agents, and Decentralized Control* [Preprint].
- Tilman, D. *et al.* (2011) 'Global food demand and the sustainable intensification of agriculture', *Proceedings of the National Academy of Sciences of the United States of America*, 108(50), pp. 20260–20264. Available at: <https://doi.org/10.1073/pnas.1116437108>.
- Vieira, M.A. *et al.* (2012) 'Object Based Image Analysis and Data Mining applied to a remotely sensed Landsat time-series to map sugarcane over large areas', *Remote Sensing of Environment*, 123, pp. 553–562. Available at: <https://doi.org/10.1016/J.RSE.2012.04.011>.
- Xue, J. and Su, B. (2017) 'Significant remote sensing vegetation indices: A review of developments and applications', *Journal of Sensors*, 2017. Available at: <https://doi.org/10.1155/2017/1353691>.
- Yin, H. *et al.* (2012) 'How Normalized Difference Vegetation Index (NDVI) Trends from Advanced Very High Resolution Radiometer (AVHRR) and Système Probatoire d'Observation de la Terre VEGETATION (SPOT VGT) Time Series Differ in Agricultural Areas: An Inner Mongolian Case Study', *Remote Sensing*, 4(11), pp. 3364–3389. Available at: <https://doi.org/10.3390/rs4113364>.
- Yogender *et al.* (2022) 'Deforestation analysis using Random Forest and interactive supervised classification approach', *IOP Conference Series: Earth and Environmental Science*, 1064(1). Available at: <https://doi.org/10.1088/1755-1315/1064/1/012028>.